Vascular Immunotargeting to Endothelial Surface in a Specific Macrodomain in Alveolar Capillaries

JUAN CARLOS MURCIANO, D. WIN HARSHAW, LUCIAN GHITESCU, SERGEI M. DANILOV, and VLADIMIR R. MUZYKANTOV

Institute for Environmental Medicine and Department of Pharmacology, University of Pennsylvania, Philadelphia, Pennsylvania; Department of Pathology and Cell Biology, University of Montreal, Montreal, Quebec, Canada; Department of Anesthesiology, University of Illinois at Chicago, Chicago, Illinois

A novel 85 kD glycoprotein (gp85) is a marker of the avesicular zone, a thin part of pulmonary endothelial cells separating alveolar and vascular compartments and lacking vesicles. This report presents the first evaluation whether mAb 30B3, a monoclonal antibody to gp85, can be used for targeting of drugs to the surface of lung endothelium. ^{125}I-mAb 30B3 accumulated in isolated perfused lungs (IPL) (22.8 $\pm$ 1.1 versus 0.5 $\pm$ 0.1 %ID/g for ^{125}I-IgG) and accumulated preferentially in the lungs after intravenous or intraarterial injection (10.9 $\pm$ 0.7 and 11.0 $\pm$ 1.5 versus 0.9 $\pm$ 0.2 %ID/g for ^{125}I-IgG). ^{125}I-mAb 30B3 uptake in IPL was rapid (T1/2 15 min), saturable (B_{max} appr. 10^5 molecules/cell), specific (inhibited by nonlabeled mAb 30B3) and temperature independent (26.3 $\pm$ 2.1 versus 22.8 $\pm$ 1.1 %ID/g at 6° C versus 37° C). Biotinylated mAb 30B3 permitted subsequent accumulation of perfused avidin derivative in IPL. Because these data indicated that mAb 30B3 binds to an accessible, poorly internalizable antigen in the lung, we conjugated mAb 30B3 with a plasminogen activator, ^{125}I-tPA. After intravenous injection in rats, lung-to-blood ratio was 8.4 $\pm$ 0.9 for mAb 30B3/^{125}I-tPA versus 0.4 $\pm$ 0.1 for IgG/^{125}I-tPA, indicating that mAb 30B3 may deliver drugs, which was supposed to exert therapeutic action in the vascular lumen (e.g., antithrombotic proteins), to the surface of pulmonary endothelium.

Keywords: endothelium; tPA; endocytosis; fibrinolysis; rats; drug delivery; lung

Vascular immunotargeting is a modern strategy designed for preferential delivery of drugs conjugated with affinity carriers to endothelial cells (1–3). Several candidate carriers have been proposed, including antibodies directed against angiotensin-converting enzyme, ACE (1, 4, 5), thrombomodulin (6), platelet-endothelial cell adhesion molecule-1, PECAM-1 (7, 8), intercellular adhesion molecule-1, ICAM-1 (9) and caveoli-associated antigens (3, 10). Lung is a privileged vascular target that contains roughly a third of endothelium in the body and receives whole cardiac output of venous blood. Therefore, antibodies directed against "pan-endothelial" antigens (e.g., anti-PECAM) provide preferential pulmonary targeting primarily because of absolute perfusion and accessibility of the pulmonary endothelium (7, 8). Antibodies against antigens that selectively enriched in the lung vasculature (e.g., anti-ACE) afford an additional degree of pulmonary selectivity of the targeting (1, 4, 5, 11, 12).

Recognition of target determinants on the cells is the first phase of the targeting strategies. The subcellular addressing represents the next phase, especially important in the context of delivery such specific and potent drugs as enzymes and genetic materials. Many endothelial surface antigens are involved in a relatively rapid dynamic endocytosis from the surface of the plasmalemma (13). Interestingly, immunotargeting to PECAM-1, an antigen that is normally poorly internalized by endothelium, is not effective either in the perfused lungs or in vivo, unless anti-PECAM carriers are modified in a way that facilitates internalization (8, 11). Internalizable carriers (e.g., modified anti-PECAM and internalizable antibodies against ACE and thrombomodulin (2, 14)) are preferable for the intracellular delivery of drugs and genes.

Theoretically, noninternalizable endothelial antigens represent a unique class of targets that could provide stable and prolonged association of drugs with endothelial surface because of the lack of disappearance from the lumen. This maneuver would be useful for delivery of antithrombotic drugs and other agents exerting the therapeutic activity in the lumen. However, targeting to the poorly internalizable endothelial antigens has not been specifically addressed in animal models.

In this study we investigated for the first time whether gp85, a recently described antigen localized in the avesicular zone of alveolar endothelium, can be used for such a surface immunotargeting. Avesicular zone is a specific plasma membrane macrodomain in the pulmonary vasculature, a thin part of endothelial cell that separates vascular and alveolar compartments and lacks vesicular machinery for endocytosis (15). Vesicular transport plays an important role in endothelial endocytosis and exocytosis (13). For example, endothelial uptake of albumin, at least in part, occurs via caveoli and vesicular trafficking pathway (10, 16). The fact that gp85 antigen is localized in the avesicular zone implies that this endothelial determinant may be poorly internalizable and thus useful for delivery of drugs to the luminal surface of endothelium. In order to test this hypothesis, we studied uptake of mAb 30B3, a monoclonal antibody against gp85, in the perfused rat lungs and in intact animals. The results shown in the report support our hypothesis and imply that mAb 30B3 can be useful for immunotargeting to the endothelial surface in the lungs.

METHODS

Reagents

The following materials were used: iodogen from Pierce (Rockford, IL), Na^{125}I from Perkin Elmer (Boston, MA), the sulfo-N-hydrohysuccinimido Nanogold and the HQ silver™ enhancement kit were from Nanoprobes, Inc. (Stony Brook, NY), fatty acid-free bovine serum albumin (BSA) from Boehringer-Mannheim (Indianapolis, IN), dimethyl formamide (DMF), mouse IgG from Sigma (St. Louis, MO), neutravidin (NA) and 6-biotinylaminocaproic acid N-hydroxysuccinimide ester (BLCNHS) from Pierce, indocarbocyanate Cy-3-conjugated goat antimouse IgG from Jackson ImmunoResearch Laboratories (West Grove, PA), and human recombinant tPA (Activase) from

Genentech Inc. (San Francisco, CA). The ECL kit was from Boehringer Mannheim/Roche Diagnostics (Laval, QC, Canada).

Monoclonal Antibodies

Three monoclonal antibodies have been produced by immunizing mice with endothelial plasmalemma obtained from rat lungs perfused with silica beads (17): (1) mAb 21D5 to gp68 or PV-1, a plasmalemmal vesicle protein associated with caveolar stomata (18, 19); (2) mAb 28D5 to a rat isoform of PECAM-1 (18, 20); and, (3) mAb 30B3 to gp85 (18). Anti-ACE mAb 9B9 that binds to rat angiotensin-converting enzyme, accumulates in the rat lungs and undergoes internalization in the endothelial cells, was described previously (9, 14, 21). Anti-PECAM mAb 62 conjugated with streptavidin was described in a recent publication (8).

Biotinylation and Radiolabeling Proteins

Proteins were biotinylated at tenfold molar excess of fresh BLCNHS and labeled with ^{125}Iodine using Iodogen as described previously (22). The modifications provide 1-2 biotins per molecule and radioactivity of $1-5 \times 10^5$ cpm/ug, without detectable inactivation of the proteins (22, 23).

Immunofluorescent Staining

The rat lungs fixed by perfusion of 1% formaldehyde in 0.1M PBS at pH 7.2 were frozen in isopentane at $-60°$ C. Ten-micrometer cryosections were quenched in 150 mM glycin and in a mixture of 1% goat normal serum, 1% ovalbumin in PBS. The sections were sequentially incubated for 2 h in a 1/20 dilution of the primary antibody or nonspecific IgG and indocarbocyanate Cy-3-conjugated goat antimouse IgG and examined in a BioRad MRC confocal imaging system using a Cy3 filter (BioRad, Richmond, CA).

Perfusion of the Isolated Rat Lung

In all animal experiments, male Sprague-Dawley rats weighing 170 to 200 g were anesthetized intraperitoneally with sodium pentobarbital (50 mg/kg). Isolated lungs were constantly perfused with a recirculating buffer and ventilated with a humidified gas mixture containing 5% CO_2 and 95% air (Airco Inc., Philadelphia, PA) in a water-jacketed chamber maintained at indicated temperature (37° C or 6° C) as previously described (9, 11, 14). Ventilation was done at 60 cycles/min, 2-ml tidal volume, 2 cm H_2O end-expiratory pressure, using a SAR-830 rodent ventilator (CWE Inc., Ardmore, PA). Perfusion through the pulmonary artery with 45 ml Krebs-Ringer buffer (KRB at pH 7.4 containing 10 mM glucose and 3% fatty acid-free BSA, KRB-BSA) was maintained by a peristaltic pump at a constant flow rate of 10 ml/min. Unless indicated otherwise, one microgram of ^{125}I-labeled mAb was added to the perfusate and after 1 h recirculating perfusion (except the kinetics studies) the lungs were perfused for 5 min with a nonrecirculating antibody-free buffer to eliminate nonbound material. The lungs were rinsed with saline, blotted with filter paper, lung wet weight was determined, and residual ^{125}Iodine was measured in a gamma-counter and expressed as percentage of perfused radioactivity per lung.

In vivo Administration of Radiolabeled Antibodies

A design, protocol, and analysis of a typical experiment have been described previously (4, 8, 11). Briefly, anesthetized male Sprague-Dawley rats were injected with a mixture of 1 μg ^{125}I-mAb 30B3 and ^{131}I-IgG via the tail vein and killed 1 h later to obtain the internal organs, which were washed with saline, blotted dry, and weighed and radioactivity in organs was determined in a gamma-counter. The parameters of ^{125}I-mAb biodistribution were calculated including % of injected dose per gram of tissue (%ID/g). This parameter permits comparisons of uptake in different organs and evaluates tissue selectivity of an antibody uptake. Without normalization per weight, uptake in large organs (liver) may look extremely large when compared with that in a relatively smaller organ (e.g., lung or heart). The ratio between %ID/g in an organ of interest and that in blood gives localization ratio (LR). This parameter compensates for a difference in blood level of circulating antibodies (e.g., because of different rate of renal or hepatic clearance or uptake by targets), helps to account for the level of nonspecific IgG in an organ and allows a more objective comparison of targeting between different carriers. The ratio between levels of an antibody and control IgG (the Immunospecificity Index [ISI], which can be calculated using either %ID/g or LR) shows the specificity of an antibody uptake when compared with nontargeted IgG.

Ultrastructural Localization of gp85 in the Lungs

Pre-embedding staining was performed as previously described (18). Briefly, sections 100 to 150 μm thick were cut from a rat lung fixed in periodate-lysine-paraformaldehyde (PLP), quenched in 20 mM glycine and 1% BSA and incubated overnight with mAb 30B3 conjugated to sulfo-N-hydroxy-succinimido Nanogold as described (18). The staining was enhanced by silver, and the specimens were embedded in Epon and examined in a Philips 400 electron microscope.

## Immunoblotting of gp85 and Caveolin in Endothelial Plasma Membranes

The endothelial membranes were isolated from perfused rat lung and heart using silica bead technique and characterized for purity immunochemically and by electron microscopy, as described previously (18, 20). Thirty micrograms of the endothelial membranes were resolved by 10% acrylamide SDS-PAGE (Minigel) and transferred to nitrocellulose filter. The upper part of the nitrocellulose filter, corresponding to high molecular weight proteins of approximately 60 to 160 kD, was incubated with anti-gp85 mAb 30B3 (1:200 dilution). The lower part of the nitrocellulose filter, corresponding to low molecular weight proteins of approximately 10 to 40 kD, was incubated with a mouse mAb directed against caveolin (1:1,000 dilution, a gift from Dr. J. Glenney, Glentech Inc., Lexington, KY). Monoclonal antibodies bound the nitrocellulose were revealed by peroxidase-conjugated goat antibody directed against mouse Ig (1:20,000; Amersham, Oakville, ONT, Canada), with an enhancement using a ECL chemiluminescence kit (Amersham).

RESULTS

In the present work we characterized the targeting capacity of monoclonal antibodies directed against surface endothelial antigens separated from rat lungs using the silica bead method developed by Jacobson and coworkers (17). The following antibodies were used: (1) mAb 21D5 to gp68 or PV-1, a novel plasmalemmal vesicle protein associated with endothelial caveolar stomata (19, 20,); (2) mAb 28D5 to a rat isoform of PECAM-1 (20); (3) mAb 30B3 to gp85, a recently described endothelial surface glycoprotein localized in the avesicular zone of the lung alveolar capillaries (18). We compared pulmonary uptake of these antibodies with a murine monoclonal antibody directed against angiotensin-converting enzyme, anti-ACE mAb 9B9. Properties of this highly promising candidate affinity carrier for the intracellular immunotargeting of drugs to endothelium are described in the literature (4, 11, 21).

An immunofluorescent study showed that mAb 30B3, as well as mAb 21D5 and mAb 28D5, provides staining of the rat lung tissue sections (Figure 1). However, only mAb 30B3 accumulated in the isolated rat lungs when perfused through the pulmonary vasculature (Figure 2). Pulmonary uptake of ^{125}I-labeled mAb 30B3 achieved 20 to 25% of injected dose per gram of lung tissue (%ID/g), a value similar to that of anti-ACE mAb 9B9, used as a positive control in this study. In contrast, the uptake of mAb 21D5 and 28D5 did not exceed that of control ^{125}I-IgG used as a negative control (0.5 ± 0.2 %ID/g).
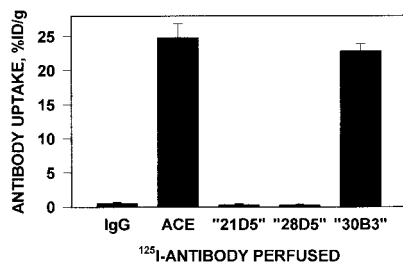
Because ^{125}I-mAb 30B3 accumulated in the isolated lungs, we characterized its tissue distribution in vivo after intravascular injection in intact rats. ^{125}I-mAb 30B3 accumulated preferentially in the lungs after intravenous injection, whereas its level in blood and in other major organs (except kidney) did not exceed that of ^{125}I-IgG (Figure 3, Panel A). Therefore, Immunospecificity Index (ISI$_{%ID/g}$, determined as ratio of ^{125}I-mAb 30B3 %ID/g to that of ^{125}I-IgG) did not exceed 1 in any organ, except kidney (renal ISI$_{%ID/g}$ is 1.7) and, most impressively, in the lungs (pulmonary ISI$_{%ID/g}$ exceeds 10). However,
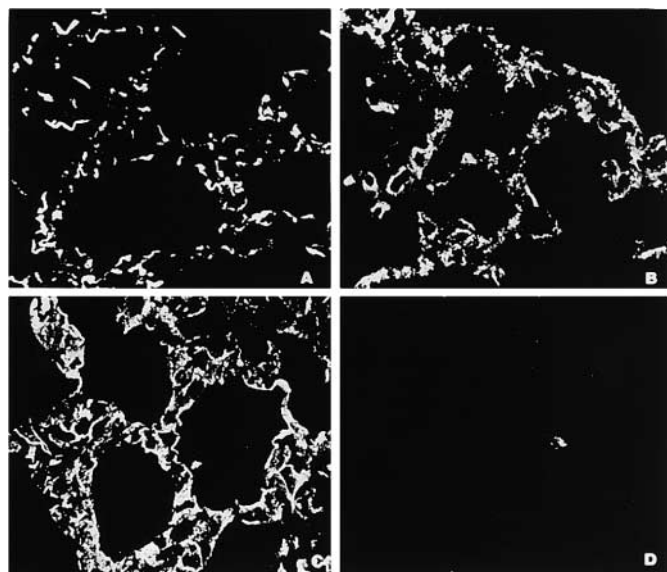
Figure 1. Immunofluorescent labeling of the rat lung tissue sections with the 30B3 (*A*), 21D5 (*B*), and 28D5 (*C*) monoclonal antibodies. As a control, sections were incubated with the secondary Cy3-conjugated antibody against mouse IgG (*D*).
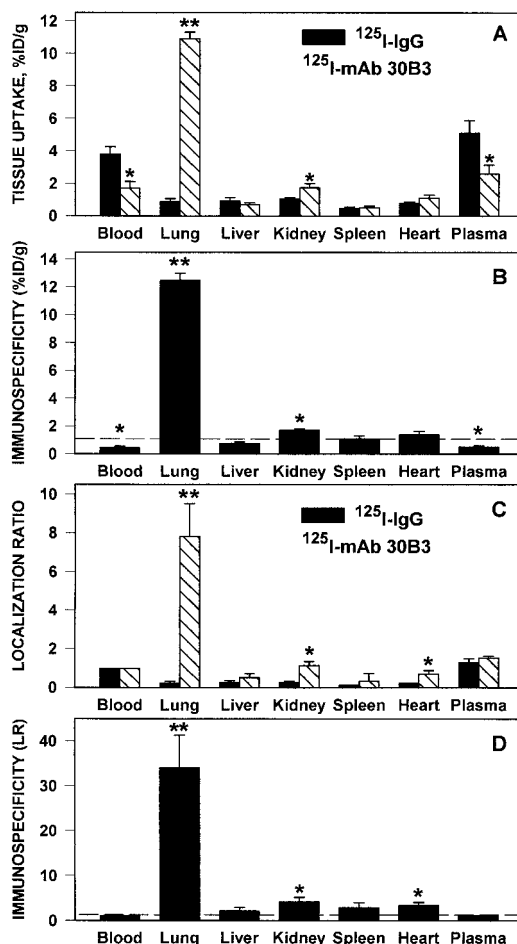

blood level of ^{125}I-mAb 30B3 was significantly lower than that of ^{125}I-IgG (Figure 3A). Similar effect has been observed with other endothelial antibodies and reflects a partial depletion of the circulating antibody pool, likely caused by binding to the target (11). In order to compensate for differences in blood level, we determined Localization Ratio for ^{125}I-mAb 30B3 and ^{125}I-IgG (Figure 3, Panel C). In the lungs, Localization Ratio of ^{125}I-mAb 30B3 was close to 10, whereas that of ^{125}I-IgG did not exceed 0.3. Renal and cardiac LR values for ^{125}I-mAb 30B3 were equal to 1.2 and 0.7 (statistically different from corresponding ^{125}I-IgG values). Thus, ISI calculated using LR reveals some degree of specific uptake of ^{125}I-mAb 30B3 in the heart (cardiac ISI_{LR} was close to 2.5), in addition to that in kidney (renal ISI_{LR} was close to 3.5). However, the pulmonary ISI_{LR} of ^{125}I-mAb 30B3 exceeded 30, thus indicating a preferential pulmonary targeting (Figure 3D).

In order to address the mechanism of preferential pulmonary accumulation of mAb 30B3 in rats, we compared its binding to purified endothelial membrane fraction that has been separated from the perfused rat lungs and hearts by silica bead technique. It can be seen in Figure 4 that antibody against caveolin, a marker antigen localized in endothelial caveoli in diverse organs, bound to the membranes purified from either lung and heart, with a slight preference to the cardiac mem-

Figure 3. Tissue distribution of ^{125}I-mAb 30B3 and control ^{125}I-IgG 1 h after systemic injection in intact anesthetized rats. Panel A shows tissue uptake of ^{125}I-IgG (*closed bars*) and ^{125}I-mAb 30B3 (*hatched bars*) expressed as %ID/g. Panel B shows $ISI_{\%ID/g}$ calculated from the data shown in Panel A. The dashed line shows ISI level equal to 1 reflecting equal tissue level of the immune and nonimmune counterparts. Panel C shows Localization Ratio, or organ-to-blood ratio of ^{125}I-IgG (*closed bars*) and ^{125}I-mAb 30B3 (*hatched bars*). Panel D shows ISI_{LR} calculated from the data shown in Panel C. The dashed line shows ISI level equal to 1. Differences between mAb 30B3 and IgG are statistically significant at **p < 0.01 or *p < 0.05.

branes. By contrast, anti-gp85 mAb 30B3 displayed an abundant binding to the pulmonary endothelial membranes and rather modest binding to the cardiac membranes. This result indicates that the pulmonary endothelium is enriched in gp85.

Preferential pulmonary targeting of intravenously injected endothelial antibodies may reflect, at least in part, the first-pass phenomenon. In order to address this issue, we compared targeting of antibodies to endothelial antigens gp85, ACE,

Figure 2. Uptake of ^{125}I-labeled monoclonal antibodies in the isolated rat lungs perfused with blood-free buffer. Antibodies (10 μg each) were perfused for 1 h and nonbound excess antibodies were eliminated by 1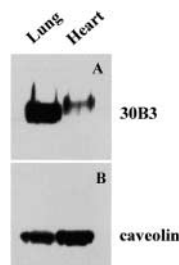0-min nonrecirculating perfusion of antibody-free buffer. ^{125}I-anti-ACE mAb 9B9, which has been described to accumulate in the rat lungs (26), was used as a positive control. ^{125}I-IgG was used as a negative control. In this and other figures the data shown are M + SEM, n = 3, unless specified.

Figure 4. Detection of the gp85 antigen in the purified endothelial membranes of the rat lung and heart. Immunoblotting with anti-gp85 mAb 30B3 and anticaveolin mAb was performed as described in METHODS. Note the significantly lower presence of the gp85 in the heart endothelial plasma membrane, contrary to the caveolar marker.
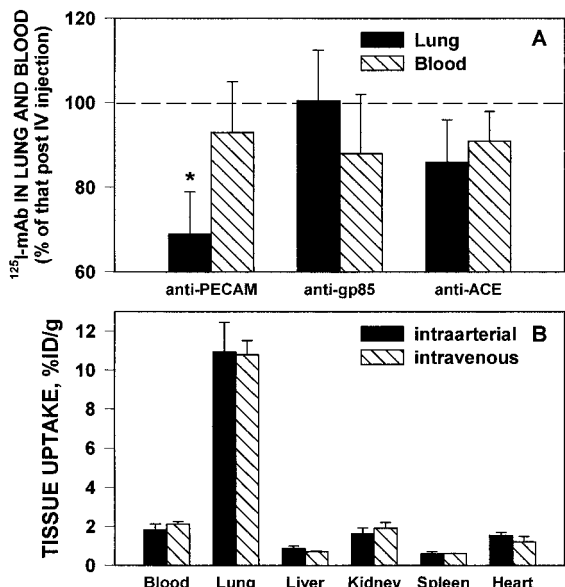
Figure 5. The administration route does not affect the pulmonary targeting of mAb 30B3 in rats. Panel A shows pulmonary uptake (*closed bars*) and blood level (*hatched bars*) of ^{125}I-labeled antibodies directed against PECAM-1, gp85 (mAb 30B3), and ACE in rats. The data obtained after intraarterial injection are presented as percent of the corresponding values obtained after intravenous injection. The difference between two routes is statistically significant at *$p < 0.05$. Panel B shows tissue uptake of ^{125}I-mAb 30B3 injected intraarterially (*closed bars*) or intravenously (*hatched bars*).

and PECAM-1 (in a form of conjugate with streptavidin) after venous versus arterial administration. Figure 5A shows that the blood level (hatched bars) and pulmonary uptake (closed bars) of these mAbs 1 h postarterial injection, expressed as percent of the corresponding level observed after intravenous injection (dash lane, 100%). In this series, blood level of all tested antibodies was slightly lower after arterial injection than that after venous injection. The nature of this effect is obscure, yet the differences with intravenous route did not reach statistical significance. The pulmonary uptake of anti-PECAM ^{125}I-mAb/streptavidin conjugate was significantly lower after arterial than after venous injection (reduced by 25%, $p < 0.05$). This result reveals significant contribution of the first-passage phenomenon in the preferential pulmonary accumulation of an antibody directed against this "pan-endothelial" antigen. By contrast, pulmonary uptake of anti-gp85 ^{125}I-mAb

30B3 after arterial injection was practically the same as after venous administration. Pulmonary uptake of anti-ACE mAb 9B9 after arterial injection was slightly (insignificantly) lower than that after venous injection. Compared with peripheral counterpart, the pulmonary capillaries were enriched in ACE (11, 12). Therefore, the data shown in Figure 5A imply that the first-pass phenomenon has very limited, if any, impact on the preferential pulmonary targeting of anti-gp85 mAb 30B3 and that the selectivity of its pulmonary uptake is similar to that of anti-ACE mAb 9B9. It can be seen in Figure 5B that the biodistribution of ^{125}I-mAb 30B3 was similar after intravenous versus intraarterial administration in all inspected tissues. It can be seen in Table 1 that ^{125}I-mAb 30B3 displayed equal uptake throughout the lung lobes regardless of the pathway of administration.

These results imply that mAb 30B3 may be useful for vascular immunotargeting of drugs to the pulmonary endothelium. Therefore, we characterized its binding to endothelium in the isolated rat lung in more detail. Addition of nonlabeled mAb 30B3 to the perfusate buffer markedly suppressed pulmonary uptake of ^{125}I-labeled mAb 30B3 in a dose-dependent manner (Figure 6, Panel A). This competition experiment confirms the specificity of mAb 30B3 immunotargeting mediated by its binding to gp85, and Figure 6B shows the binding curve of ^{125}I-mAb 30B3 in IPL. Practical reasons limited the total number of experimental points and the highest mAb 30B3 concentration attained in this setting. Therefore, the quantitative analysis of the binding data obtained in IPL should be interpreted more cautiously than that of binding curves obtained in standard RIA using immobilized purified
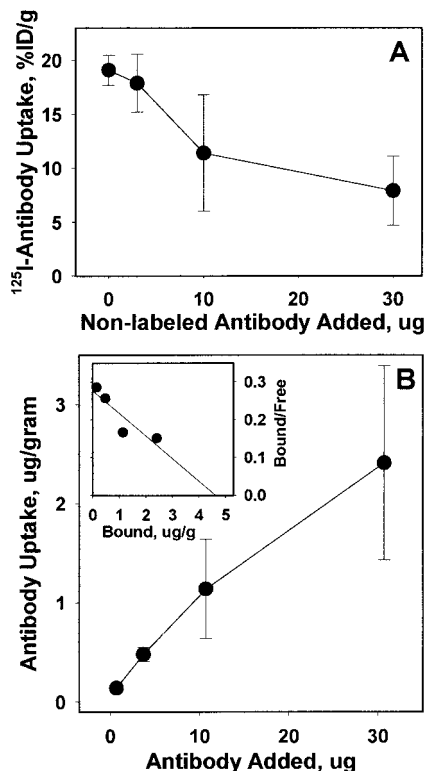
TABLE 1. DISTRIBUTION OF ^{125}I-LABELED mAb 30B3 IN THE RAT LUNG LOBES ONE HOUR AFTER ADMINISTRATION IN THE PERFUSED RAT LUNGS OR SYSTEMIC ADMINISTRATION IN INTACT RATS*

| Lung Lobe	IPL	IV	IA
Right Low	23.3 ± 0.8	11.2 ± 1.3	10.5 ± 2.1
Right Middle	20.7 ± 0.9	9.8 ± 0.5	12.5 ± 1.1
Right Upper	19.5 ± 0.9	11.3 ± 0.3	13.2 ± 1.8
Cardiac	24.1 ± 1.2	8.9 ± 0.3	15.4 ± 2.5
Left	21.4 ± 1.1	12.5 ± 2.3	9.7 ± 1.8

* Radiolabeled mAb 30B3 (1–2 µg) was administered in the isolated perfused lung (IPL) or injected intravenously (IV) or in the left ventricle (intraarterial, IA) as described in the Methods. The data are presented as percent of injected dose per gram of tissue (M ± SEM, n = 3). There was no statistically significant difference between the lobes at each pathway of administration. Note that there is no extrapulmonary uptake of mAb 30B3 in the isolated lung during perfusion (for example, by reticuloendothelial system, excretory organs and lymphatic system). This helps to explain a higher uptake of mAb 30B3 in the isolated lungs when compared with that after systemic (IV and IA) administration.

Figure 6. Binding of ^{125}I-mAb 30B3 in perfused rat lungs. Panel A shows inhibition of pulmonary uptake of ^{125}I-mAb 30B3 (1 µg) by addition of the indicated dose of nonlabeled mAb 30B3 to the perfusate buffer. Panel B shows dose dependence of the pulmonary uptake of ^{125}I-mAb 30B3 and a pilot Scatchard analysis of the binding curve (insert).
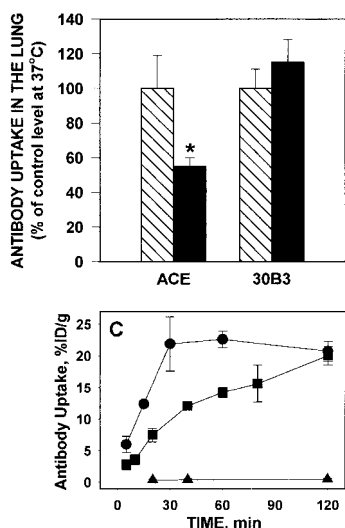
Figure 7. Comparison of the pulmonary uptake of ^{125}I-mAb 30B3 and ^{125}I-mAb 9B9 in the perfused rat lungs. *Panel A.* Effect of the temperature on the uptake (37° C, *hatched bars*, 6° C, *closed bars*). The uptake of ^{125}I-mAb 30B3 at 6° C was similar to that at 37° C, whereas uptake of the internalizable ^{125}I-mAb 9B9 was suppressed by 50% at 6° C. The data are shown as mean ± SEM, n = 6 for mAb 9B9 at 37° C, n = 3 for other groups. *Panel B.* Kinetics of the antibodies uptake. The uptake of ^{125}I-mAb 30B3 reached rapid saturation (*circles*, T1/2 = 15 min), whereas that of ^{125}I-mAb 9B9 was markedly slower (*squares*, T1/2 = 60 min). There was no uptake of nonspecific ^{125}I-IgG in the entire period of perfusion (*triangles*).

antigens. However, the Scatchard analysis of the ^{125}I-mAb 30B3 binding curve (the insert in Figure 6B) implies that the antibody possesses a high binding affinity (K_d approximately 2.5 nM) and that its total binding capacity (Bmax) approaches 4.5 μg per rat lung, or approximately 1.5×10^{13} molecules per gram of rat lung. Because rat lung contains approx. 4×10^8 endothelial cells (24), this result implies that a single "generic" endothelial cell in the rat lung possesses approximately 10^5 binding sites for mAb 30B3.

In the next series, we have compared the temperature dependence and kinetics of ^{125}I-labeled mAb 30B3 uptake in the perfused rat lungs with those of ^{125}I-labeled anti-ACE mAb 9B9. The equilibrium level of ^{125}I-mAb 30B3 in the perfused rat lungs in these series was consistent with that shown in Figure 6. The uptake of mAb 30B3 was not suppressed by low temperature (6° C) that inhibits an energy-dependent internalization, whereas it suppressed the uptake of internalizable mAb 9B9 (Figure 7, Panel A); Figure 7, Panel B, shows that mAb 30B3 displayed a very rapid saturation of the uptake, whereas mAb 9B9 displayed markedly slower uptake (T1/2 was 15 min for mAb 30B3 versus 60 min for mAb 9B9). These results imply that mAb 30B3 does not undergo rapid internalization in the pulmonary vasculature.

In order to characterize the subcellular localization of mAb 30B3 antigen in the rat lungs more precisely, we stained lung tissue sections with mAb 30B3 covalently coupled to 1.2 nm organometallic gold nanoparticles. Identical qualitative results were obtained with either the preembedding and postembedding approaches, except that in the latter, the intensity of staining was substantially lower. This is a known consequence of the fact that in postembedding method only the antigens "sticking out" of the resin in the plane of the section are available to the immune reagents. On the other hand, this technique can probe cellular and tissue compartments impermeable to antibodies in the pre-embedding variant. Examination of the tissue sections in a transmission electron microscope revealed that mAb 30B3 binds exclusively to vascular endothelium in the lung tissue. Pulmonary epithelial cells were free of gold particles and only a few particles could be detected in the interstitium. It can be seen in Figure 8 that in the alveolar capillaries, mAb 30B3 bound specifically to a thin part of endothelial cell body that lacks vesicles and separates alveolar and

vascular compartments (i.e., avesicular zone) (15). In a sharp contrast, plasma membrane covering endothelial nuclear and paranuclear regions containing majority of the organelles and plasmalemmal vesicles was practically free of labeling. Major fraction of the gold particles was associated with the luminal surface of endothelial plasmalemma in the avesicular zone, with only few particles detectable intracellularly or in subendothelial compartment.

The results shown in Figures 7 and 8 imply that mAb 30B3 recognizes an easily accessible epitope on a relatively poorly internalizable surface endothelial antigen, gp85, localized in the plasma membrane domain that lacks endocytotic machinery. Therefore, this antibody may be useful for the vascular immunotargeting of drugs, which supposed to persist on the endothelial surface and act in the blood (e.g., antithrombotic agents). In order to evaluate this avenue, we studied delivery of tissue-type plasminogen activator (tPA) coupled to mAb 30B3 using avidin-biotin crosslinker. Our previous work documented that tPA retains full fibrinolytic activity after such modification (23).

In the first series, we perfused isolated rat lungs for 1 h with 100 μg of biotinylated mAb 30B3. After elimination of nonbound material and change of the perfusate buffer, we further perfused 20 μg of ^{125}I-labeled biotinylated tPA conjugated with neutravidin (^{125}I-tPA/NA complex). In this setting, the pulmonary uptake of ^{125}I-tPA/NA was 9.1 ± 1.8 %ID/g. Uptake of ^{125}I-tPA/NA perfused after control biotinylated IgG was five times lower (1.6 ± 0.4 %ID/g) and did not exceed that of ^{125}I-tPA in control perfused rat lungs (1.8 ± 0.5 %ID/g). Specific uptake of ^{125}I-tPA/NA in the lungs perfused postaccumulation of biotinylated mAb 30B3 confirms the notion that pulmonary endothelium poorly internalizes mAb 30B3. Otherwise, biotinylated mAb 30B3 would disappear from the lumen and could not harbor ^{125}I-tPA/NA conjugate to endothelium. We have demonstrated previously that avidin does not bind in the isolated rat lungs when perfused after the internalizable biotinylated anti-ACE mAb 9B9 (14).
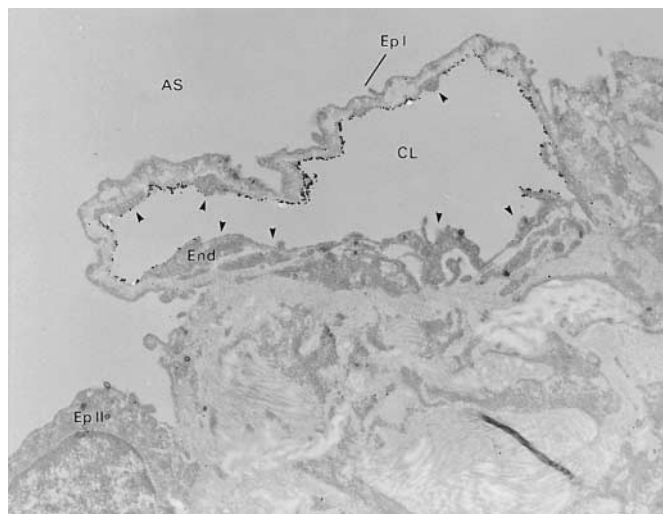
Figure 8. Labeling of rat lung tissue section with Nanogold-conjugated mAb 30B3. Endothelial plasma membrane indicated with arrowheads. Note the unique association of the corresponding antigen to the attenuated, avesicular domain of the capillary endothelium. Other parts of endothelial cell body, thick enough to contain caveolae or other organelles, lack or contain markedly less gold particles. The surface of epithelial cells (EPI and EPII) is completely free of gold particles. AS = air space; CL = capillary lumen; End = endothelial cell.

To evaluate whether mAb 30B3 carrier permits drug targeting *in vivo*, we studied tissue distribution of ^{125}I-tPA/NA conjugated with biotinylated mAb 30B3 in intact rats. The conjugate displayed higher hepatic and renal uptake than mAb 30B3 (Figure 9). This result is similar to that seen with tPA coupled to other carriers and can be attributed to tPA-mediated clearance of the conjugates (23). However, tPA coupled with mAb 30B3, but not with control nonspecific IgG, preferentially accumulated in the lungs after intravenous injection in intact rats. Localization ratio was 8.4 ± 0.9 for mAb 30B3/^{125}I-tPA versus 0.4 ± 0.1 for IgG/^{125}I-tPA. Nonconjugated tPA displayed even lower pulmonary uptake and extremely fast elimination from the bloodstream than control IgG/tPA conjugate (not shown). The mAb 30B3/^{125}I-tPA Immunospecificity Index (ratio between the tissue uptake of immune and nonimmune counterparts) exceeded 1 only in the lungs. Thus, $ISI_{\%ID/g}$ was equal to 13, whereas ISI_{LR}, compensating for the difference in blood clearance, exceeded 20. This result indicates that mAb 30B3 provides vascular immunotargeting of tPA to the lungs.

DISCUSSION

This study has addressed immunotargeting of drugs to a recently described antigen (gp85) localized in the endothelial avesicular zone in the alveolar capillaries. We employed perfusion of isolated rat lungs and systemic administration in intact rats in order to study the targeting of antibodies to the surface endothelial antigens obtained from rat pulmonary endothelium by silica bead separation (18, 20). Our results show that mAb 30B3 to gp85 accumulates in the rat lungs and permits immunotargeting of drugs to the pulmonary vasculature. Two other monoclonal antibodies produced by immunizing mice by a similar preparation of rat lung endothelial plasmalemma displayed intense staining of the lung tissue, yet failed to accumulate either in the perfused rat lungs (Figure 2) and *in vivo* (not shown). Lack of mAb 28D5 targeting (that recognizes rat PECAM-1 isoform) is not entirely surprising in the light of the finding that, unless coupled to an optimal size vehicle, PECAM antibodies poorly accumulate in the lungs (8, 11). A likely explanation for mAb 21D5 failure is that its epitope in PV-1 antigen is not accessible for the antibody from the lumen.

We compared pulmonary targeting of mAb 30B3 with that of anti-ACE mAb 9B9, a well-characterized internalizable carrier potentially useful for intracellular delivery of drugs and genes to the pulmonary endothelium (4, 11, 14). Binding of mAb 30B3 to vascular endothelium is similar to that of anti-ACE mAb 9B9 by several parameters. A pilot Scatchard analysis of binding in the perfused rat lungs revealed that mAb 30B3 possesses slightly higher affinity (2.5 nM) and lower number of binding sites (10^5 molecules/cell) than mAb 9B9 (10 nM and 2.5×10^5 molecules/cell) (14). However, in contrast to ACE antibodies, mAb 30B3 is poorly internalizable in the lungs. This conclusion is based on the following findings: (*1*) binding of mAb 30B3 is not suppressed at low temperature that prohibits internalization; (*2*) pulmonary uptake of mAb 30B3 is very rapidly saturated; and, (*3*) biotinylated mAb 30B3 is exposed to the lumen after perfusion and binds subsequently perfused avidin. An apparent lack of mAb 30B3 intracellular uptake corroborates with a unique localization of gp85 in the endothelial plasma membrane. Electron microscopy shows a unique localization of mAb 30B3 antigen in the pulmonary capillaries, where it is restricted to the avesicular zone that lacks major organells and endocytotic vesicles.

Analysis of tissue distribution and targeting of radiolabeled antibodies in intact animals can be performed in many ways.
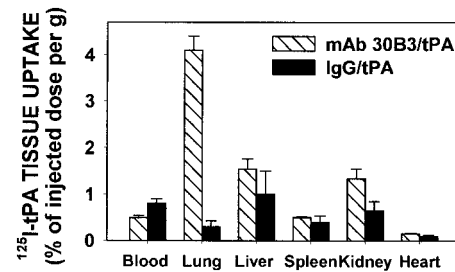
Figure 9. Pulmonary immunotargeting of tPA by mAb 30B3. Tissue distribution of ^{125}I-tPA/NA complex conjugated with either biotinylated mAb 30B3 (*hatched bars*) or with biotinylated IgG (*closed bars*) 1 h after intravenous injection in intact anesthetized rats. The data are presented as percent of injected dose per gram.

In order to analyze the selectivity of mAb targeting to organs of interest, it would be tempting to normalize mAb uptake per surface vascular area in an organ. However, published data on surface vascular area in the organs are fragmentary and conflicting. For example, the vascular surface area in the lungs varied from 38 m^2 (25) to 300 m^2 (17) and even 5,000 m^2 (26) in humans and from 2,500 cm^2/g of lung (27) to 4,800 cm^2/g (28) in rats (normalized to 300 g per rat). In addition, the uptake of ^{125}I-labeled antibodies in many organs was hardly distinguishable from that of control IgG (presumably reflecting antigen-independent uptake such as Fc-receptor-mediated binding). These circumstances precluded an accurate quantification of the organ selectivity of specific targeting. However, the goal of our work was to develop a drug delivery strategy, not to define the degree of tissue selectivity of expression of blood-accessible gp85 in the vasculature. Therefore, we utilized standard pharmacokinetics parameters (%ID/g and organ/blood ratio, LR), which permit an accurate comparison between target and nontarget uptake of different agents. A relatively high pulmonary uptake of any given antibody could reflect the fact that the lung vascular area is larger than that in other organs. However, comparison of a mAb pulmonary uptake with that of nonspecific control IgG (Immunospecificity Index, ISI) shows the specificity of preferential pulmonary uptake of mAb 30B3 (and anti-ACE mAb 9B9). Some degree of selective uptake was also noted in the kidney and heart, although the specific cardiac accumulation of mAb 30B3 could not be revealed without account for the difference in blood clearance of the antibody and IgG. The immunoblotting data indicate that pulmonary vasculature is enriched in gp85 and help to explain a relative selectivity of the preferential pulmonary uptake of mAb 30B3 (Figure 4). Noteworthy, mAb 30B3 did not accumulate in the liver and spleen, in contrast to antibodies directed against other endothelial antigens, such as PECAM and ICAM (11).

Analysis of pulmonary uptake after intravenous versus intraarterial administration provides an additional insight into the preferential pulmonary uptake of mAb 30B3. Thus, the uptake of an antibody directed against PECAM-1 was reduced by roughly 30% after arterial injection, indicating that the first-pass phenomenon represents a substantial component in pulmonary targeting directed to this pan-endothelial antigen. In contrast, pulmonary uptake of anti-ACE was only marginally and statistically insignificantly affected by arterial routing, likely reflecting specifically high presentation of ACE in the pulmonary capillaries, documented recently in humans and rats (11, 12). Thus, the fact that pulmonary uptake of 30B3 was equal after either route implies that selectivity of its pulmonary accumulation at least matches that of anti-ACE. In

addition, mAb 30B3 shows a relatively more selective pulmonary uptake than antibodies to pan-endothelial antigens PECAM-1 or ICAM-1, which also accumulate in the liver and spleen (*see also* 11, 29).

The selectivity of endothelial immunotargeting represents an intriguing issue that is a subject of ongoing studies. Endothelial cells display morphologic, biochemical, and antigenic heterogeneity in the vascular system (30–33). Identification of the surface endothelial markers of specific domains in the vasculature may be used for a more selective vascular immunotargeting. First, normal endothelial cells localized in different organs vary in marker antigens (30). Although such organ-specific antigens remain to be identified for many organs, results of recent studies obtained using *in vivo* selection of phage display libraries imply that unique surface determinants exist in brain, lung, spleen, and many other organs (33). Second, endothelial cells localized in different type of vessel express different markers. For example, capillary endothelium is enriched in HEMCAM and CD36 antigens (34, 35), whereas venous endothelium is enriched in LuECAM antigen (36). Third, certain antigens are heterogeneously distributed in the endothelial plasmalemma. For example, PV-1 antigen and caveolin are associated with caveoli (17, 19), whereas PECAM-1, at least in cell culture, tends to be concentrated in the intercellular borders (37). Finally, endothelial cells involved in pathologic process such as tumor growth or inflammation, express abnormal antigens such as inducible surface adhesion molecules and growth factors and their receptors. Antibodies against these determinants have been proposed for recognition of specific endothelial determinants in tumors and inflammation foci (3, 38, 40). Antigenic heterogeneity of endothelial cells may provide an invaluable tool for selective addressing of drugs in the vasculature (vascular immunotargeting) (2).

So far, endothelial antigenic heterogeneity has been addressed mostly by staining of tissue sections. This approach permits maximal exposure of target antigens and thus reveals a whole repertoire of specific markers in the vasculature. However, in order to be a good candidate target for drug delivery, a marker must bind circulating carriers in the vascular domain of interest. Such a binding is governed by a carrier affinity, as well as by surface density and accessibility of a marker determinant to the blood. Accessibility to biotinylating or iodinating agents (40, 41) does not necessarily mean that a membrane protein is a good target since its specific epitopes may be poorly accessible for such large drug carriers as antibodies, liposomes, or viral particles. Our previous studies with diverse radiolabeled antiendothelial antibodies injected in intact animals documented that tissue level of a target antigen is a less important determinant for an antibody accumulation than epitope accessibility to the bloodstream (1, 4, 11).

There are very few, if any, examples of domain-specific carriers in the literature. Antibodies to caveoli-associated antigens bind to this specific domain in the endothelial plasmalemma and may permit intraendothelial and transendothelial delivery of drugs (3). The targeting profile of antibodies directed against caveoli is worth more detailed investigation. Speculatively, PECAM-1 antibodies provide another example of domain-specific targeting since PECAM-1 is localized in intracellular borders in endothelial cell culture (9). However, PECAM-1 seems to be more uniformly distributed on the endothelial luminal surface *in vivo* (42).

Vascular immunotargeting to the antigens localized in specific vascular domains in the lungs, such as gp85, has not been addressed directly in the literature. Several groups approached the problem via studies of morphologic and functional heterogeneity of the normal and pathologically altered pulmonary

endothelial cells (10, 25, 41). Studies using membrane protein mapping (41), phage display (33), and isolation of endothelial antigens by silica beads (3, 18, 20, 39, 43) provided several targets potentially useful for recognition of and drug delivery to specific endothelial domains in the lungs. However, none of the potential carrier antibodies directed against these targets has been characterized in terms of binding to endothelium, subcellular uptake and drug delivery in the perfused lungs and intact animals. Therefore, to our knowledge, this study provides the first evidence that a monoclonal antibody against an antigen localized in a unique macrodomain in the alveolar endothelium affords vascular immunotargeting of drugs to the lungs. Strategic location of the mAb 30B3 antigen implies that this poorly internalizable carrier may be useful for targeting of antithrombotic agents (such as tPA) or agents that would intercept and inactivate proinflammatory mediators diffusing from alveolar to vascular compartments.

Carrier antibodies may modulate function, membrane metabolism and shedding of target antigens. Thus, some ACE antibodies suppress its enzymatic activity (21, 44), whereas PECAM antibodies inhibit adhesion of white blood cells (45). Such effects may represent either side effect or secondary benefit for a therapy. Thus, further consideration of mAb 30B3 as a drug carrier depends on identification of the antigen and its function. This pending information is important in the context of the vascular immunotargeting and better understanding of nature of endothelial functional heterogeneity.

References

1. Danilov SM, Sakharov I, Martynov A, Faerman A, Muzykantov VR, Klibanov A, Trakht IN. Monoclonal antibodies to ACE: a powerful tool for lung and vessel studies. *J Mol Cell Cardiol* 1989;21:165–170.
2. Muzykantov VR. Immunotargeting of drugs to the pulmonary vascular endothelium as a therapeutic strategy. *Pathophysiology* 1998;5:15–33.
3. Schnitzer JE. Vascular targeting as a strategy for cancer therapy. *N Engl J Med* 1998;339:472–474.
4. Danilov SM, Muzykantov VR, Martynov A, Atochina E, Sakharov I, Trakht IN, Smirnov VN. Lung is a target organ for monoclonal antibody to ACE. *Lab Invest* 1991;64:118–124.
5. Muzykantov V, Puchnina E, Martynov A, Danilov S. *In vivo* administration of glucose oxidase conjugated with monoclonal antibody to ACE: targeting into the lung. *Am Rev Respir Dis* 1989;136:1464–1473.
6. Kennel S, Lee R, Bultman S, Kabalka G. Rat monoclonal antibody distribution in mice: an epitope inside the lung vascular space mediates very efficient localization. *Nucl Med Biol* 1990;17:193–200.
7. Li S, Tan Y, Viroonchatapan E, Pitt BR, Huang L. Targeted gene delivery to pulmonary endothelium by anti-PECAM antibody. *Am J Physiol* 2000;278:L504–511.
8. Muzykantov VR, Cristofidou-Solomidou M, Balyasnikova I, Harshaw D, Schultz L, Fisher A, Albelda S. Streptavidin facilitates internalization and pulmonary uptake of an anti-endothelial cell antibody (PECAM-1): a strategy for vascular immunotargeting of drugs. *Proc Natl Acad Sci USA* 1999;96:2379–2384.
9. Atochina EN, Balyasnikova IV, Danilov SM, Granger DN, Fisher AB, Muzykantov VR. Immunotargeting of catalase to ACE or ICAM-1 protects perfused rat lungs against oxidative stress. *Am J Physiol* 1998;27519:L806–L817.
10. Schnitzer JE, Carley WW, Palade GE. Albumin interacts specifically with a 60-kDa microvascular endothelial glycoprotein. *Proc Natl Acad Sci USA* 1988;85:6773–6777.
11. Danilov S, Gavrilyuk V, Franke F, Pauls K, Harshaw D, McDonald T, Miletich D, Muzykantov V. Lung uptake of antibodies to endothelial antigens: key determinants of vascular immunotargeting. *Am J Physiol* 2001;280:L1335–L1347.
12. Franke F, Metzger R, Bohle R, Kerkman L, Alhenc-Gelas F, Danilov SM. Angiotensin-I-converting enzyme (CD143) on endothelial cells in normal and in pathological conditions. In: Kishimoto T, *et al.* Leuko-

cyte typing VI. White cell differentiation antigens. New York: Garland Publishing Inc.; 1997. p. 749–751.

13. Niles WD, Malik AB. Endocytosis and exocytosis events regulate vesicle traffic in endothelial cells. *J Membrane Biol* 1999;167:85–101.

14. Muzykantov VR, Atochina E, Kuo A, Barnathan E, Notarfrancesco K, Shuman H, Dodia C, Fisher A. Endothelial cells internalize monoclonal antibody to ACE. *Am J Physiol* 1996;270:L704–L713.

15. Simonescu D, Simonescu M. Differential distribution of the cell surface charge on the alveolar capillary unit. Characteristic paucity of anionic sites on the air-blood barrier. *Microvasc Res* 1983;25:85–100.

16. Tiruppathi C, Song W, Bergenfeldt M, Sass P, Malik AB. gp60 activation mediates albumin transcytosis in endothelial cells by tyrosine kinase-dependent pathway. *J Biol Chem* 1997;272:25968–25975.

17. Jacobson BS, Schnitzer JE, McCaffery M, Palade GE. Isolation and partial characterization of the luminal plasmalemma of microvascular endothelium from rat lungs. *Eur J Cell Biol* 1992;58:296–306.

18. Ghitescu L, Jacobson B, Crine P. A novel, 85-kDa endothelial antigen differentiates plasma membrane macrodomain in lung alveolar capillaries. *Endothelium* 1999;6:241–250.

19. Stan RV, Ghitescu L, Jacobson BS, Palade G. Isolation, cloning and localization of rat PV-1, a novel endothelial caveolar protein. *J Cell Biol* 1999;145:1189–1198.

20. Ghitescu LD, Crine P, Jacobson B. Antibodies specific to the plasma membrane of rat lung microvascular endothelium. *Exp Cell Res* 1997; 232:47–55.

21. Balyasnikova IV, Moldobaeva AK, Miletich DJ, Danilov SM. Monoclonal antibodies to ACE accelerate the proteolytic cleavage of ACE from the cell surface in a epitope-dependent manner (abstract). *Circulation* 1998;98(Suppl):I-607.

22. Muzykantov VR, Atochina E, Ischiropoulos H, Danilov S, Fisher AB. Immunotargeting of antioxidant enzymes to the pulmonary endothelium. *Proc Natl Acad Sci USA* 1996;93:5213–5218.

23. Muzykantov VR, Barnathan E, Atochina E, Kuo A, Danilov S, Fisher AB. Targeting of antibody-conjugated plasminogen activators to the pulmonary vasculature. *J Pharmacol Exp Ther* 1996;279:1026–1034.

24. Crapo J, Barry B, Foscue H, Shelburne J. Structural and biochemical changes in rat lungs occurring during exposures to lethal and adaptive doses of oxygen. *Am Rev Respir Dis* 1980;122:123–144.

25. Crone C. The permeability of capillaries in various organs as determined by use of the 'indicator diffusion' method. *Acta Physiol Scand* 1963; 58:292–305.

26. Davis MG, Hagen P-O. The vascular endothelium. *Ann Surg* 1993;218: 593–609.

27. Crapo J, Barry B, Gehr P, Bachhoffen M, Weibel E. Cell number and cell characteristics of the normal human lung. *Am Rev Respir Dis* 1982; 125:332–337.

28. Vock R, Weibel ER. Massive hemorrhage causes changes in morphometric parameters of lung capillaries and concentration of leukocytes in microvasculature. *Exp Lung Res* 1993;19:559–577.

29. Panes J, Perry M, Anderson D, Manning A, Leone B, Cepinskas G, Rosenbloom C, Miyasaka M, Kvietis P, Granger DN. Regional differ-

30. Auerbach R, Alby L, Morrissey LW, Tu M, Joseph J. Expression of organ-specific antigens on capillary endothelial cells. *Microvasc Res* 1985; 29:401–411.

31. Garlanda C, Dejana E. Heterogeneity of endothelial cells. Specific markers. *Arterioscler Thromb Vasc Biol* 1997;17:1193–1201.

32. Gerritsen M. Functional heterogeneity of vascular endothelial cells. *Biochem Pharmacol* 1987;36:2701–2711.

33. Rajotte D, Arap W, Hagedorn M, Koivinen E, Pasqualini R, Ruoslahti E. Molecular heterogeneity of the vascular endothelium revealed by in vivo phage display. *J Clin Invest* 1998;102:430–437.

34. Greenwalt DE, Lipsky RH, Ockenhouse CF, Ikeda H, Tandon NN, Jameison GA. Membrane glycoprotein CD36: a review of its roles in adherence, signal transduction, and transfusion medicine. *Blood* 1980; 80:1105–1115.

35. Vainio O, Dunon D, Assisi F, Dangy JP, McNagny KM, Imhof BA. HEMCAM, an adhesion molecule expressed by c-kit hemopoietic progenitors. *J Cell Biol* 1996;135:1655–1668.

36. Goetz DJ, el-Sabbah ME, Hammer DA, Paul BU. LuECAAM-1 mediated adhesion of melanoma cells to endothelium under conditions of flow. *Int J Cancer* 1996;65:192–199.

37. Newman PJ. The Biology of PECAM-1. *J Clin Invest* 1997;99:3–7.

38. Huang X, Molema G, King S, Watkins L, Edgington T, Thorpe PE. Tumor infarction by antibody-directed targeting of tissue factor to tumor vasculature. *Science* 1997;275:547–550.

39. Keelan E, Licence S, Peters A, Binns R, Haskard D. Characterization of E-selectin expression *in vivo* with use of a radiolabeled monoclonal antibody. *Am J Physiol* 1994;266:H279–290.

40. De La Fuente EK, Dawson CA, Nelin LD, Bongard RD, McAuliff TL, Merker MP. Biotinylation of membrane proteins accessible via the pulmonary circulation in normal and hyperoxic rats. *Am J Physiol* 1997;272:L461–L479.

41. Merker M, Carley WW, Gillis CN. Molecular mapping of pulmonary endothelial membrane glycoproteins on the intact rabbit lung. *FASEB J* 1990;4:3040–3048.

42. Scholz D, Schaper J. PECAM-1 is localized over the entire plasma membrane of endothelial cells. *Cell Tissue Res* 1997;290:623–631.

43. Jacobson B, Stolz DB, Schnitzer JE. Identification of endothelial cell-surface proteins as targets for diagnosis and treatment of disease. *Nat Med* 1996;2:482–484.

44. Danilov S, Atochina E, Hiemish H, Churakova T, Moldobayeva A, Sakharov I, Deichman G, Ryan U, Muzykantov VR. Interaction of monoclonal antibody to angiotensin-converting enzyme (ACE) with antigen *in vitro* and *in vitro* and *in vivo*: antibody targeting to the lung induces ACE antigenic modulation. *Intern Immunol* 1994;6:1153–1160.

45. Vaporician AA, DeLisser HM, Yan HC, Mendiguren I, Thom SR, Jones ML, Ward PA, Albelda SM. Platelet-endothelial cell adhesion molecule-1 (PECAM-1) is involved in neutrophil recruitment *in vivo*. *Science* 1993;262:1580–1582.

ences in constitutive and induced ICAM-1 expression in vivo. *Am J Physiol* 1995;269:H1955–H1964.